AGU PUBLICATIONS

JGR

Journal of Geophysical Research: Biogeosciences

RESEARCH ARTICLE
10.1002/2015JG002980

Key Points:
- Start of season maximum leaf chlorophyll and LAI values differed by 41 days
- Daily GPP showed the strongest relationship with canopy chlorophyll content
- LAI overestimated GPP at the start of the growing season

Correspondence to:
H. Croft,
holly.croft@utoronto.ca

Citation:
Croft, H., J. M. Chen, N. J. Froelich, B. Chen, and R. M. Staebler (2015), Seasonal controls of canopy chlorophyll content on forest carbon uptake: Implications for GPP modeling, *J. Geophys. Res. Biogeosci.*, *120*, 1576–1586, doi:10.1002/2015JG002980.

Received 2 MAR 2015
Accepted 23 JUN 2015
Accepted article online 26 JUN 2015
Published online 14 AUG 2015

Seasonal controls of canopy chlorophyll content on forest carbon uptake: Implications for GPP modeling

H. Croft[1], J. M. Chen[1], N. J. Froelich[2], B. Chen[1,3], and R. M. Staebler[4]

[1]University of Toronto, Department of Geography, Toronto, Ontario, Canada, [2]Northern Michigan University, Department of Earth, Environmental and Geographical Sciences, Marquette, Michigan, USA, [3]International Institute for Earth System Science, Nanjing University, Nanjing, China, [4]Air Quality Processes Research Section, Environment Canada, Toronto, Ontario, Canada

Abstract Forested ecosystems represent an important part of the global carbon cycle, with accurate estimates of gross primary productivity (GPP) crucial for understanding ecosystem response to environmental controls and improving global carbon models. This research investigated the relationships between leaf area index (LAI) and leaf chlorophyll content (Chl_{Leaf}) with forest carbon uptake. Ground measurements of LAI and Chl_{Leaf} were taken approximately every 9 days across the 2013 growing season from day of year (DOY) 130 to 290 at Borden Forest, Ontario. These biophysical measurements were supported by on-site eddy covariance flux measurements. Differences in the temporal development of LAI and Chl_{Leaf} were considerable, with LAI reaching maximum values within approximately 10 days of bud burst at DOY 141. In contrast, Chl_{Leaf} accumulation only reached maximum values at DOY 182. This divergence has important implications for GPP models which use LAI to represent the fraction of light absorbed by a canopy (fraction of absorbed photosynthetic active radiation (fAPAR)). Daily GPP values showed the strongest relationship with canopy chlorophyll content (Chl_{Canopy}; $R^2 = 0.69$, $p < 0.001$), with the LAI and GPP relationship displaying nonlinearity at the start and end of the growing season ($R^2 = 0.55$, $p < 0.001$). Modeled GPP derived from LAI × PAR and Chl_{Canopy} × PAR was tested against measured GPP, giving $R^2 = 0.63$, $p < 0.001$ and $R^2 = 0.82$, $p < 0.001$, respectively. This work demonstrates the importance of considering canopy pigment status in deciduous forests, with models that use $fAPAR_{LAI}$ rather than $fAPAR_{Chl}$ neglecting to account for the importance of leaf photosynthetic potential.

1. Introduction

Terrestrial ecosystems absorb approximately 120 Gt yr^{-1} of carbon, from the atmosphere by plants through photosynthesis [*Grace*, 2004], which is the process by which solar radiation is converted into chemical energy through chemical reactions in leaf chloroplasts. Forests represent an important part of the global carbon cycle and of annual carbon budgets, with an estimated net global forest C sink of 1.1 (±0.8) Gt C yr^{-1} [*Pan et al.*, 2011]. Accurate estimates of gross primary productivity (GPP) at a range of spatial and temporal scales, and for different vegetation types, are critical for understanding ecosystem response to increased atmospheric CO_2 levels and to improve carbon cycle modeling [*Intergovernmental Panel on Climate Change*, 2013]. The importance of photosynthetic carbon uptake to carbon budgets means that any uncertainty in GPP is a primary concern in global carbon cycle modeling. This uncertainty arises partly from a lack of mechanistic understanding due to the difficultly in measuring photosynthesis continuously and over large spatial extents. Currently, a unique GPP model that can be applied over different terrestrial ecosystems and wide-ranging environmental conditions remains elusive [*Coops et al.*, 2010; *Hilker et al.*, 2008; *Rossini et al.*, 2012]. Perhaps the most widely used approach to model GPP from remote sensing data is the light use efficiency (LUE) concept [*Monteith*, 1972, 1977], which incorporates the potential of converting the fraction of absorbed photosynthetic active radiation (fAPAR) into biomass: GPP = LUE × fAPAR × PAR. LUE therefore represents the efficiency of the conversion of absorbed energy to fixed carbon [*Monteith*, 1972]. Within satellite-based production efficiency models [*Ruimy et al.*, 1996; *Running et al.*, 2004], fAPAR is often represented using a linear or nonlinear function of a biomass-sensitive vegetation index (i.e., fAPAR = a + b × normalized difference vegetation index (NDVI)), as a proxy for the total leaf area (leaf area index (LAI)) [*Xiao et al.*, 2004]. However, not all absorbed light results in carbon assimilation. In optimum conditions approximately 80% of absorbed light is used in photosynthesis, although this can be as low as 0%, depending on light conditions, environmental

factors (e.g., water and nutrient availability), and physiological status [*Buschmann*, 2007]. Leaf chlorophyll content (Chl_{Leaf}) is the "photosynthetic apparatus" of the plant [*Peng et al*., 2013], with only the PAR absorbed by chlorophyll being used for photosynthesis [*Zhang et al*., 2009]. Chl_{Leaf} is therefore related mechanistically to vegetation productivity [*Zhang et al*., 2005]. As a consequence, it is important to differentiate between canopy biomass and leaf function, particularly from remotely sensed products where canopy "greenness" is an amalgamation of canopy structure and leaf pigment content. Research has shown that in deciduous forests, while leaf expansion occurs very rapidly, with LAI reaching maximum values within approximately 10 days of bud burst, Chl_{Leaf} takes longer to increase [*Gond et al*., 1999; *Keenan et al*., 2014], lagging LAI by approximately 30 days [*Croft et al*., 2014b]. However, the consequence of this seasonal divergence in LAI and Chl_{Leaf} on the conversion of absorbed PAR to fixed carbon is largely unexplored. In cropland environments, researchers have found a close relationship between canopy chlorophyll content (Chl_{Canopy}) and GPP [*Gitelson et al*., 2003, 2006; *Peng et al*., 2011]. However, crops have a different growth cycle and phenology to deciduous forests, with planted crops experiencing coincident increases in LAI and Chl_{Leaf} as the plants grow. Using satellite data, *Harris and Dash* [2010] demonstrated that a chlorophyll-sensitive vegetation index (Medium-Resolution Imaging Spectrometer (MERIS) Terrestrial Chlorophyll Index) showed stronger correlations with daily GPP for a range of vegetation types than the biomass-sensitive enhanced vegetation index (EVI).

Tower-based eddy covariance measurements allow the investigation of carbon fluxes in forest ecosystems across different time scales, in response to both meteorological conditions and biophysical drivers [*Baldocchi et al*., 2001; *Barr et al*., 2007]. Accurate flux data are crucial to the understanding of forest ecophysiological processes and for the development and validation of ecosystem models [*Baldocchi*, 2008; *Barr et al*., 2007; *Zha et al*., 2013]. This study uses eddy covariance carbon flux measurements in conjunction with ground-based sampling of LAI and Chl_{Leaf} throughout the growing season at a temperate mixed forest at Borden Forest Research Station, Ontario [*Froelich et al*., 2015]. The direct assessment of the relationship between plant physiology and forest carbon assimilation will better refine carbon modeling approaches and inform the integration of appropriate remotely sensed products in carbon models. The objectives of this study were to (1) assess the differences between Chl_{Leaf} and LAI phenology and their impact on the seasonal dynamics of forest carbon uptake and (2) improve on LAI-based GPP models through the integration of information on leaf physiological status.

2. Methods

2.1. Field Location

The Borden Forest Research Station is a mixed temperate forest located near the southern tip of Georgian Bay in southern Ontario (44°19′N, 79°56′W) in the Great Lakes/St. Lawrence forest region [*Froelich et al*., 2015]. This ecotone extends across eastern North America between 44 and 47°N and is a transition zone containing both southern temperate forest species and northern boreal species [*Goldblum and Rigg*, 2010; *Leithead et al*., 2010]. The dominant species present are red maple (*Acer rubrum*), eastern white pine (*Pinus strobus*), large-tooth aspen and trembling aspen (*Populus grandidentata* and *Populus tremuloides*), white and red ash (*Fraxinus americana* and *Fraxinus pennsylvanica*), and American beech (*Fagus grandifolia*) [*Lee et al*., 1999; *Teklemariam et al*., 2009]. Mean canopy height is 22 m, and over the last 15 years mean annual temperature at the site was 7.4°C and mean annual total precipitation was 784 mm.

2.2. Ground Data Collection

Leaves were sampled from the upper canopy of trees directly from a 44 m flux tower located at the site. Four tree species were sampled (red maple, large-tooth aspen, trembling aspen, and white ash) from which five leaves were selected per species on average every 9 days from day of year (DOY) 130 to 290. Chl_{Leaf} was measured from leaves sampled from the top of the canopy, and represents the maximum leaf chlorophyll potential for a given date, with lower values expected in understory leaves [*Zhang et al*., 2007]. The sampled branches were tagged to ensure repeatable measurements through the growing season. Leaf samples were sealed in plastic bags and kept at a temperature of 0°C for subsequent biochemical analysis to extract Chl_{Leaf}. Foliar chlorophyll was extracted using spectranalyzed grade *N*,*N*-dimethylformamide, and absorbance was measured at 663.8 nm, 646.8 nm, and 480 nm using a Cary-1 spectrophotometer [*Croft et al*., 2014a, 2013; *Wellburn*, 1994]. The measured leaf chlorophyll values for each species reported in this study

were calculated as mean values from five leaf samples per species collected on each sampling date. Total leaf chlorophyll (Chl $a+b$) content ($\mu g/cm^2$) was derived using the method reported by *Moorthy et al.* [2008]. LAI and canopy structural parameters were measured on the same days as leaf sampling. Effective LAI (*Le*) measurements were obtained using the LAI-2000 plant canopy analyzer (Li-Cor, Lincoln, NE, USA), following the methods outlined by *Chen et al.* [1997], and converted to true LAI values as follows:

$$\mathrm{LAI} = [(1-\alpha)Le\gamma_E]/\Omega_E \tag{1}$$

where α is the ratio of woody area to total area, γ_E is the ratio of needle area to shoot area, and Ω_E is the clumping index. The ratio of woody area to total area ($\alpha = 0.17$) accounts for the interception of radiation by branches and tree trunks that would lead to artificially high LAI values, and was obtained from previously published values for similar deciduous stands [*Gower et al.*, 1999]. For broadleaf species, individual leaves are considered foliage elements and γ_E is set at 1. Ω_E was measured using the TRAC (Tracing Radiation and Architecture of Canopies) instrument [*Chen and Cihlar*, 1995]. Both the LAI-2000 and TRAC measurements were collected at 10 m intervals along a 300 m transect extending from the flux tower in a north-south orientation.

2.3. Meteorological Measurements

Meteorological and eddy covariance fluxes of carbon exchange were obtained from a 44 m tall tower (see *Froelich et al.* [2015] for full details). Air temperature and relative humidity measurements were made on the tower at two heights (33 and 41 m) from a Vaisala HMP-45C sensor. Incoming photosynthetically active radiation (PAR_{in}) was measured at 41 m using Li-Cor LI-190SA sensor; downwelling PAR transmitted through the canopy (PAR_{trans}) was measured at 1.5 m using an upward pointing Li-Cor LI-191 line quantum sensor. PAR reflected by the canopy (PAR_{out}) was measured at 33 m using a Li-Cor LI-190SA sensor. The fraction of absorbed PAR (fAPAR) was calculated as follows:

$$\mathrm{fAPAR} = (\mathrm{PAR_{in}} - \mathrm{PAR_{out}} - \mathrm{PAR_{trans}})/\mathrm{PAR_{in}} \tag{2}$$

2.4. Eddy Covariance Measurements

Half hourly net ecosystem productivity (NEP) at Borden Forest was computed as $\mathrm{NEP} = -(F_{CO_2} + S_{CO_2})$ where F_{CO_2} is the covariance of vertical velocity fluctuations and CO_2 fluctuations (measured, respectively, with a sonic anemometer and a closed-path infrared gas analyzer inlet co-located at a height of 33 m) and S_{CO_2} is the storage change of carbon in the volume below the 33 m eddy covariance instruments [*Froelich et al.*, 2015]. Computation of the gas fluxes was performed as follows. Spikes that fall outside ±10 standard deviations from the mean within each 0.5 h were identified and eliminated. Mean values of the six despiked time series (three components of velocity, sonic temperature, and CO_2 and H_2O mole fractions) were computed and subtracted from the 0.5 h time series to calculate perturbation values (w', C', etc.). The CO_2 flux (F_{CO_2} [$\mu mol\,m^{-2}\,s^{-1}$]) was calculated from the WPL-corrected vertical turbulent flux of the CO_2 mole fraction $\left(\overline{w'CO_2'}_{WPL}\right)$ as

$$F_{CO_2} = \rho_{air}\overline{w'CO_2'}_{WPL}/M_{air} \tag{3}$$

where the WPL correction accounts for density effects due to water vapor fluctuations [*Webb et al.*, 1980]. The storage change, per unit area of ground in the layer below 33 m, was estimated as $S_{CO_2} = \int_0^{33m} \frac{\Delta CO_2}{\Delta t} dz$; this estimate was made using gas profile measurements when available or using the single-point measurement of CO_2 from the eddy covariance sensor at 33 m, when profile data were unavailable. The net ecosystem exchange ($\mu mol\,m^{-2}\,s^{-1}$) was calculated as the sum of F_{CO_2}, the vertical CO_2 flux at 33 m, and S_{CO_2}, the change of CO_2 storage. Horizontal turbulent fluxes and both vertical and horizontal advection of CO_2 were assumed to be negligible [*Staebler and Fitzjarrald*, 2004]. NEP data were filtered during periods of low turbulence, as diagnosed using friction velocity [*Barr et al.*, 2013]. In addition, NEP data were also filtered when winds were from directions with short fetch [*Froelich et al.*, 2015]. Following filtering, gaps in the flux data set were filled using the method of *Barr et al.* [2004]. Respiration (RE) was computed during nights or cold periods as RE = −NEP; daytime warm season RE and gaps in nighttime or cold season RE were estimated using an empirical model based on air and soil temperature. Daytime gross primary productivity

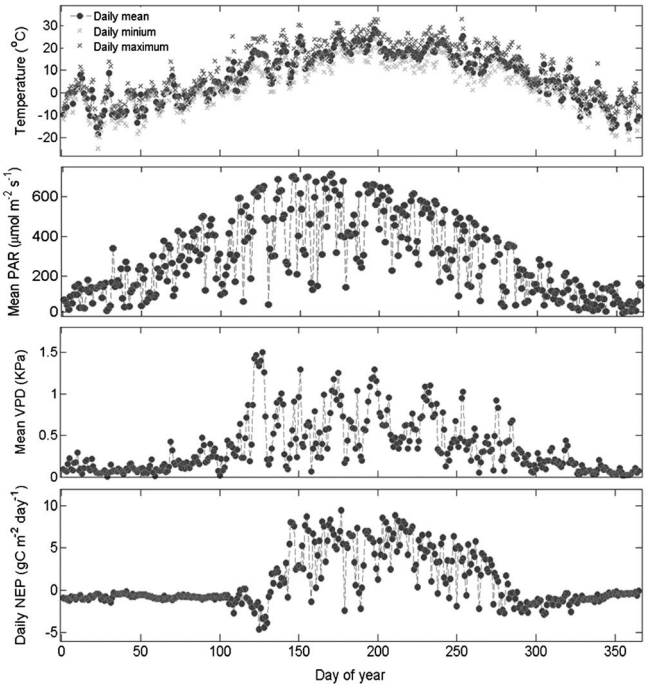

Figure 1. Daily averages of meteorological variables and daily total NEP for Borden Forest for 2013.

was computed during the daytime growing season as GPP = NEP + RE; gaps in this GPP were the estimated using an empirical model based on photosynthetically active radiation (PAR).

3. Results and Discussion

3.1. Daily Meteorological Variables and Net Ecosystem Productivity

Key meteorological variables, along with daily total NEP for the Borden Forest site in 2013, are shown in Figure 1. In this deciduous forest, moisture is not a limiting factor and temperature is primary control on carbon uptake and release through respiration [*Froelich et al.*, 2015]. PAR is needed as a source of energy and to drive light-dependent reactions in the chloroplasts which convert CO_2 into structural carbohydrates [*Ruimy et al.*, 1994]. The availability of moisture in the air indicated by the vapor pressure deficit (VPD) can affect carbon assimilation, with high VPD values resulting in stomatal closure, limiting CO_2 uptake and photosynthesis [*Farquhar and Sharkey*, 1982; *Law et al.*, 2002].

During 2013, Borden Forest experienced a minimum air temperature of −24.8°C on 23 January and a maximum temperature of 32.8°C on 10 September. Average daily winter (January–March) temperature was −3.3°C, and average daily midgrowing season (July–August) temperature was 19.8°C. PAR remained low until around DOY 50, and reached maximum daily mean values of ~700 $\mu mol\, m^{-2} s^{-1}$ during the summer months, although values show considerable variability due to the presence of cloud cover. VPD remained fairly constant until around DOY 120, when an abrupt increase coincided with a corresponding drop in NEP. The NEP figure indicates the start and end of the growing season and net carbon uptake period. The transition of the forest from a carbon source in the winter (as respiration exceeds primary production) to a carbon sink occurred around DOY 130, and the return to carbon sink in the fall occurred around DOY 280. There is considerable variability in NEP values in the middle of the growing season, with some days representing a carbon source, likely due to the inhibition of photosynthesis resulting from a reduction in incident PAR or water availability constraints [*Gonsamo et al.*, 2015].

3.2. Seasonal Dynamics of Leaf Chlorophyll Content and Leaf Area Index

The temporal differences in leaf chlorophyll content and LAI across the growing season are shown in Figure 2. Chlorophyll content is shown as a weighted average of the four sampled species based on their relative stem density in the forest (red maple 60.4%, large-tooth aspen 12.9%, trembling aspen 12.4%, and ash 14.2%). An asymmetric Gaussian model fitted to the data highlights the differences in the LAI or Chl_{Leaf} trends at the start and end of the season. Canopy photographs from a camera mounted at the top of the tower are shown along selected corresponding ground measurement dates for visual context.

The differences in the temporal development of LAI and Chl_{Leaf} are striking, with LAI reaching maximum values within approximately 10 days of bud burst and leaf expansion. In contrast, Chl_{Leaf} accumulation took substantially longer, not reaching maximum values until approximately 40 days after bud burst. The largest differences between LAI and Chl_{Leaf} occurred at DOY 141 at the start of the season. At DOY 141, LAI values were at 98% of their seasonal maximum, but Chl_{Leaf} was only at 32% of maximum values. This discrepancy is supported by the canopy photographs, which clearly show full green canopy coverage at

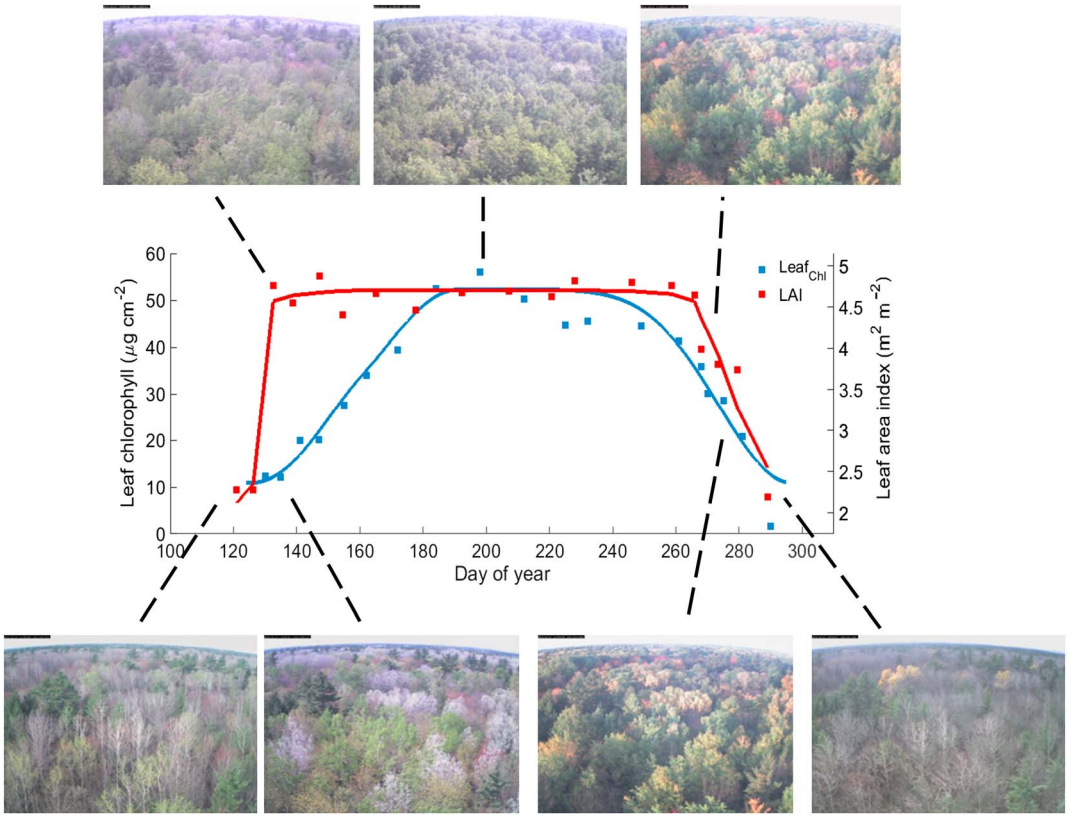

Figure 2. Variations in leaf chlorophyll content and LAI across a growing season. Individual measurements are shown with a fitted asymmetric Gaussian function. Top of canopy photographs are given alongside ground measurement dates.

DOY 141. However, ground measurements demonstrate that despite the presence of green leaves, Chl_{Leaf} was still accumulating. Chlorophyll reached within 5% of seasonal maximum values at DOY 182. The temporal divergence at the end of the growing season occurred during leaf senescence, when the leaves remain on the tree after chlorophyll production has abated and the chlorophyll present in leaves has broken down.

3.3. Leaf and Canopy Chlorophyll and LAI Variations With Carbon Flux

Given the role that chlorophyll content plays in the light harvesting reactions during plant photosynthesis, it is imperative to investigate the impact that the temporal trends of Chl_{Leaf} and LAI (Figure 2) have on forest carbon uptake, particularly at the start and end of the growing season. Chl_{Leaf}, LAI, and canopy chlorophyll (Chl_{Canopy}) values are shown against daily GPP values (Figure 3), where Chl_{Canopy} is calculated as $LAI \times Chl_{Leaf}$.

It is clear from Figure 3b that the abrupt increase in LAI at the start of the season following bud burst is not matched by daily GPP values, which are much slower to increase at the start of the growing season. This is replicated at the end of the growing season, when daily GPP begins to decrease much earlier than LAI, from a maximum rate at around DOY 200. By contrast, the GPP values show a much closer correspondence to leaf and canopy chlorophyll contents, which displays a slower increase at the start of season and declines at the end of the season that occurs earlier than decreases in LAI.

Relationships between carbon uptake and leaf chlorophyll and LAI are shown in Figure 4. While LAI and Chl_{Canopy} are fairly static in the middle of the growing season (when not under environmental stress), GPP responds to more dynamic meteorological variables, including PAR and temperature. To minimize these dynamic effects, the GPP values used are 5 day averages taken around sampling date.

Figure 4 reveals a strong linear relationship between mean daily GPP and both Chl_{Leaf} and Chl_{Canopy} ($R^2 = 0.65$, $p < 0.005$ and $R^2 = 0.69$, $p < 0.001$, respectively), confirming the trends in Figure 3. This result

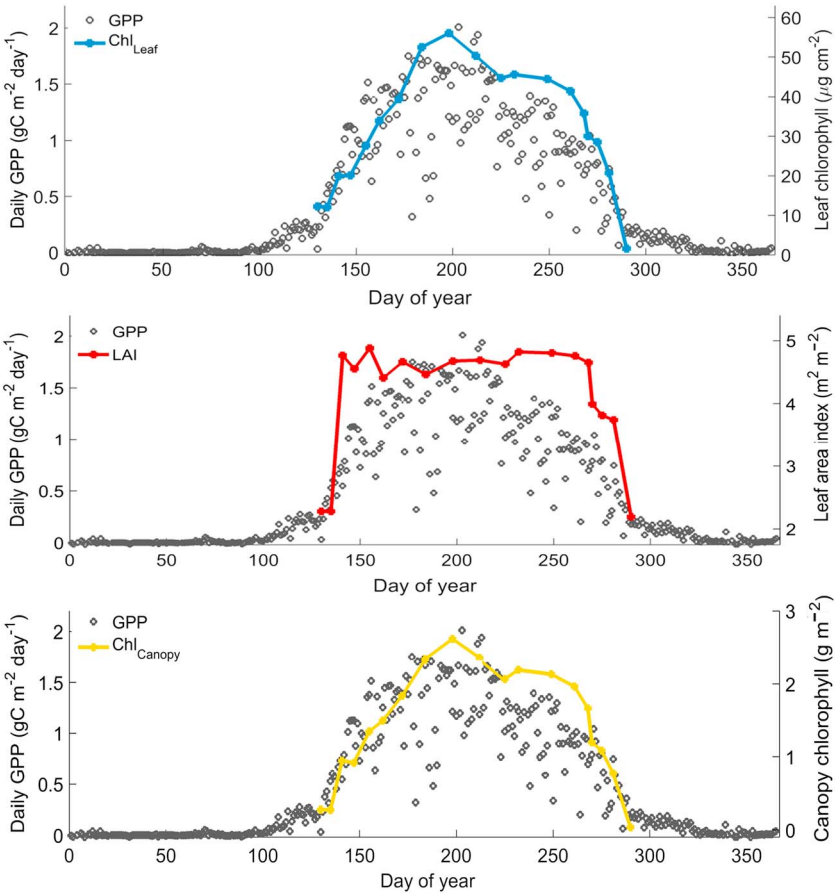

Figure 3. Daily GPP totals (g C m^{-2} d^{-1}) alongside: (first panel) leaf chlorophyll content (μg cm^{-2}), (second panel) leaf area index (m^2 m^{-2}), and (third panel) canopy chlorophyll content (μg m^{-2}).

demonstrates the importance of considering leaf/canopy pigment status, as a proxy for photosynthetic potential, when representing carbon assimilation. The central role that chlorophyll content plays in photosynthesis means that the light absorbed by leaves during time periods with suboptimal amounts of chlorophyll may not lead to carbon assimilation. Importantly, the unsuitability of using LAI as a parameter to model GPP is also highlighted (Figure 4b). Due to a lack of a mechanistic relationship between LAI and photosynthesis, the divergence between LAI and Chl_{Leaf} at the start and end of the season results in a weaker, nonlinear relationship of LAI with GPP ($R^2 = 0.55$, $p < 0.005$).

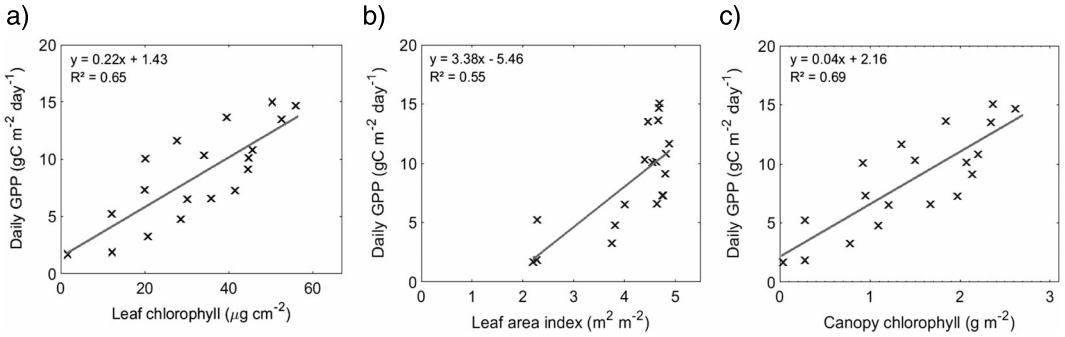

Figure 4. Mean daily GPP (gC m^{-2} d^{-1}) calculated from a 5 day window around the ground sampling date, regressed against (a) leaf chlorophyll content (μg cm^{-2}), (b) LAI (m^2 m^{-2}), and (c) canopy chlorophyll content (g m^{-2}).

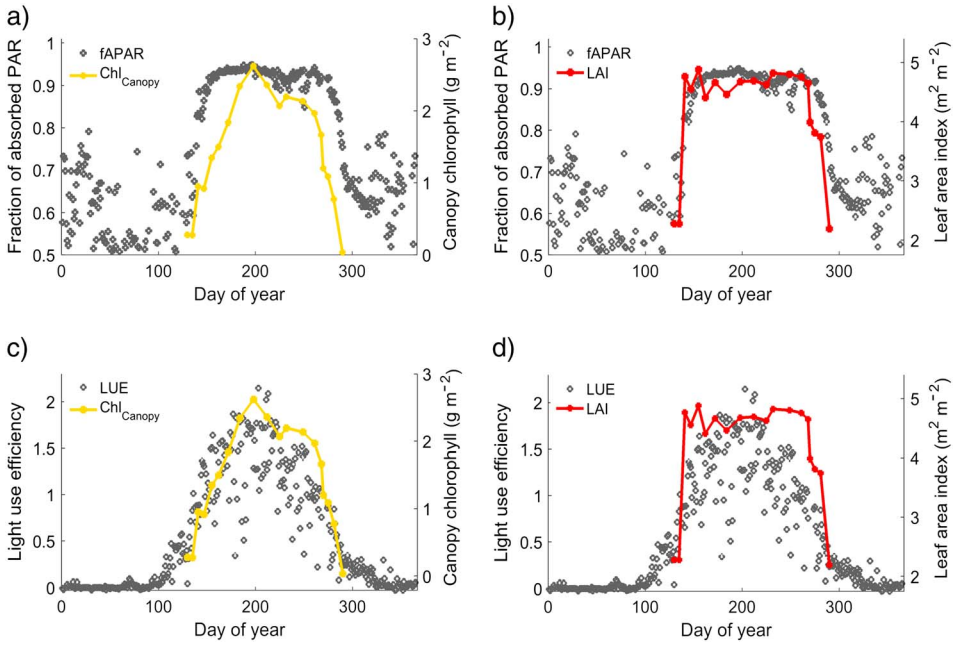

Figure 5. Temporal variation of canopy chlorophyll with (a) fAPAR and (c) LUE and LAI with (b) fAPAR and (d) LUE at Borden Forest.

3.4. The Fate of Light Absorbed by the Canopy

To further investigate the fate of light following absorption by a leaf, temporal trends in Chl_{Canopy} and LAI are compared with canopy biophysical variables used in gas exchange modeling. The fraction of absorbed PAR (fAPAR) and light use efficiency (LUE) are shown in Figure 5 with ground-measured LAI and Chl_{Canopy}. fAPAR was calculated using above and below canopy PAR sensors, as the amount of incident PAR that is absorbed by the canopy (APAR) expressed as a fraction of the downwelling radiation. fAPAR thus denotes the light absorption capacity of the canopy [*Fensholt et al.*, 2004; *Ruimy et al.*, 1994]. Canopy light use efficiency (LUE) is a measure of the conversion efficiency of absorbed light into photosynthetically fixed CO_2 [*Zhang et al.*, 2009], defined here as the ratio between CO_2 assimilation rate and APAR.

The strong temporal correlation between LAI and fAPAR (Figure 5b) indicates that light is absorbed by the canopy the entire time that leaves are present on the tree, including during senescence and during chlorophyll accumulation. However, due to the absence of chlorophyll at the start and end of the growing season (Figure 5a), this absorbed light is not used for photosynthesis. The seasonal relationship between LUE and canopy chlorophyll content illustrates the importance of the availability of the photosynthetic pigment for CO_2 fixation [*Peng et al.*, 2011; *Wu et al.*, 2009]. There is therefore an important distinction between the fraction of light absorbed by leaf area ($fAPAR_{LAI}$) and of photosynthetically active leaf area ($fAPAR_{Chl}$) [*Zhang et al.*, 2009]. fAPAR is currently a fundamental biophysical input variable in vegetation productivity models [*Fensholt et al.*, 2004]. However, while LAI is an important physical variable for modeling water and energy fluxes and for scaling between the leaf and canopy, these results indicate that in order to accurately model photosynthetic processes and thus carbon assimilation, leaf physiological status must be considered.

3.5. Modeling Gross Primary Productivity

Currently, most plant production efficiency models predict GPP as a function of LUE, fAPAR, and incident PAR, with NDVI or a similar vegetation index used to represent LAI as a proxy for fAPAR [*Zhang et al.*, 2009]. Figure 6 investigates the midday relationship between GPP with LAI × PAR and Chl_{Canopy} × PAR. LAI and Chl_{Canopy} were linearly interpolated to obtain daily midday values. Midday PAR and GPP values were calculated as mean values between 11:00 and 01:00 P.M. The data are divided into the start, middle, and end of the growing season to examine temporal effects on the relationship.

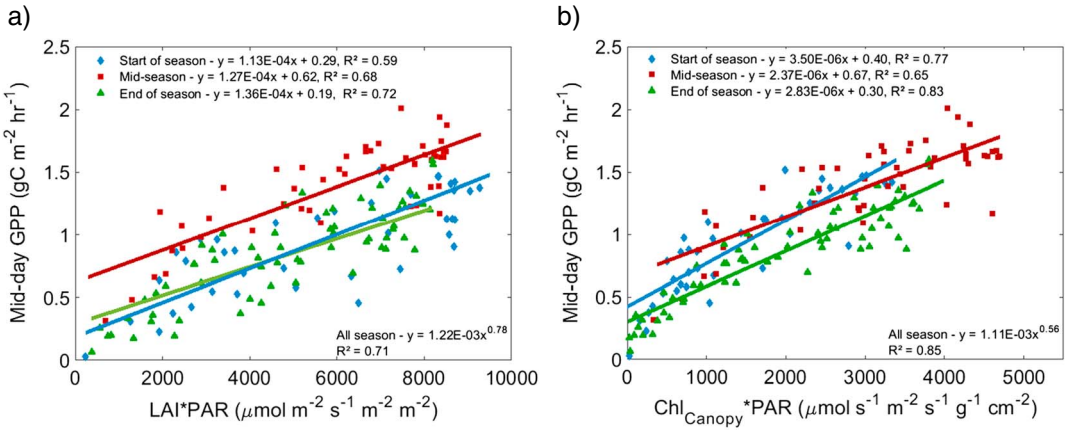

Figure 6. Relationships between mean midday GPP (gC m^{-2} h^{-1}) and (a) LAI × PAR and (b) Chl_{Canopy} × PAR, according to time of season.

Using all seasons combined, there is a stronger overall relationship between Chl_{Canopy} × PAR and GPP ($R^2 = 0.85$, $p < 0.001$) than between LAI × PAR and GPP ($R^2 = 0.71$, $p < 0.001$). The reason for the scatter in the LAI × PAR-GPP relationship can be inferred from Figure 6a, which shows the variability in data by season. In contrast to the Chl_{Canopy} × PAR relationship, the use of LAI shows a stratification based on time of year and an insensivity to LAI status. The same LAI × PAR values give a large range of GPP values, indicating that LAI is not the primary biophysical canopy variable controlling GPP.

The actual magnitude of error that arises from modeling GPP from leaf area without accounting for leaf physiology is investigated in Figure 7. The data were randomly divided equally into a calibration and validation set, with the calibration regression for LAI × PAR: $y = 0.001x^{0.81}$, $R^2 = 0.73$, $p < 0.001$ and Chl_{Canopy} × PAR: $y = 0.001x^{0.57}$, $R^2 = 0.82$, $p < 0.001$. The start of season and end of season data points are highlighted in blue and green, respectively.

The importance of a plant physiological control on GPP rates is confirmed in Figure 7, with errors in predicted GPP from LAI inputs arising at the beginning and end of the growing season (Figure 7a). The average start of season error from LAI-based midday GPP estimates is 0.27 gC m^{-2} h^{-1} and end of season error is 0.21 gC m^{-2} h^{-1}. This is in comparison to the average Chl-based modeled midday GPP error, which is −0.01 gC m^{-2} h^{-1} and 0.02 gC m^{-2} h^{-1} for the start and end of season time frames, respectively. The integration of pigment content (Chl_{Canopy}) consequently shows a marked improvement in GPP estimates, with a very strong and linear regression ($R^2 = 0.82$, $p < 0.001$), along the 1:1: line.

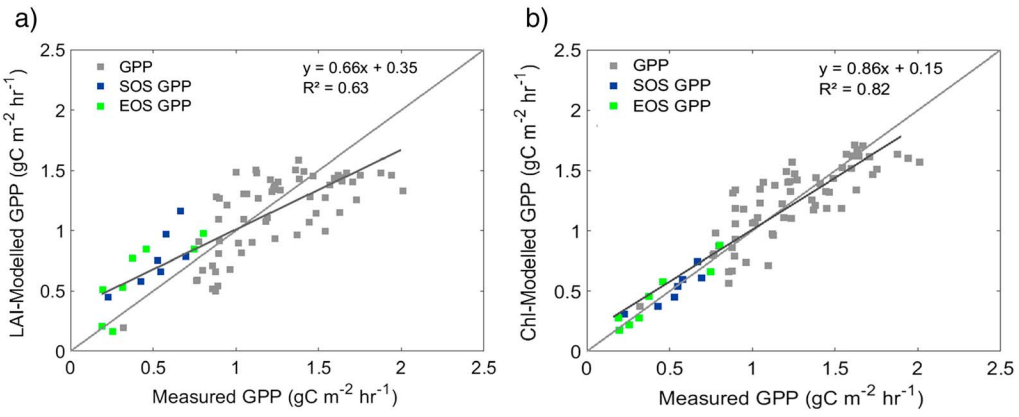

Figure 7. Modeled versus measured GPP results, according to (a) LAI × PAR and (b) Chl_{Canopy} × PAR. Start of season and end of season data points are highlighted in blue and green, respectively.

4. Discussion

This study demonstrates the strong influence of leaf physiology on forest carbon assimilation throughout a deciduous forest growing season. However, further work is required to assess the scalability of relationships shown in this paper, across different plant functional types and varying environmental conditions. Errors in the LAI-modeled GPP would be expected to be more apparent in water-limiting environments, where water stresses in the growing season would restrict GPP (and reduce chlorophyll content), but not provoke an immediate proportional response in LAI values. Further, while leaf chlorophyll content may serve as a proxy for plant photosynthetic potential, the respective response times of leaf chlorophyll content and vegetation productivity to environmental drivers and plant stress is an important factor. Mechanistic investigations between leaf chlorophyll content and photosynthetic parameters, such as maximum rates of carboxylation (Vcmax) and electron transport (Jmax) may further our ability to integrate leaf chlorophyll content into advanced ecosystem models developed for regional and global applications. Currently, a major limitation to the incorporation of leaf chlorophyll content into carbon models is the lack of accurate regional or global leaf chlorophyll products. There have been a large number of publications that have produced local-scale assessments of chlorophyll, using both empirical vegetation indices [*Croft et al*., 2014c; *Wu et al*., 2008] and physically based models [*Croft et al*., 2013; *Houborg et al*., 2009; *Zhang et al*., 2008], that have been well validated using ground measurements. The lack of progress at the global scale has largely been due to the lack of spectral bands sampled by existing satellite sensors that are sensitive to chlorophyll content, along the red-edge portion of the electromagnetic spectrum. However, recent work has indicated that physically based radiative transfer models can accurately model leaf chlorophyll content using a reduced number of spectral bands [*Croft et al*., 2015]. Furthermore, an increasing number of sensors are beginning to contain the "red-edge" bands that are highly sensitive to chlorophyll content, including Envisat MERIS (from 2002 to 2012), the forthcoming European Space Agency Sentinel-2 mission, and the Vegetation and Environment monitoring New MicroSatellite (Venus) platform. These upcoming missions will play an important role in making spatially distributed chlorophyll measurements across global scales more achievable.

5. Conclusion

The results of this study highlight the consequences of differing temporal behavior between Chl_{Leaf} and LAI on carbon uptake in a mixed temperate forest. Ground measurements indicated that LAI reached within 5% of seasonal maximum values by DOY 141, compared to Chl_{Leaf} at DOY 182. The implications of this temporal divergence in canopy physical and biochemical properties for carbon assimilation are seen in the respective relationships with daily GPP, where Chl_{Canopy} showed the strongest correlation ($R^2 = 0.69$, $p < 0.001$). The nonlinear behavior of LAI with GPP at the start and end of the growing season led to a weaker relationship with GPP ($R^2 = 0.55$, $p < 0.001$), suggesting potential errors in production efficiency models that predict GPP using LAI as a proxy for fAPAR. Modeled GPP from LAI × PAR and from $Chl_{Canopy} \times$ PAR ($R^2 = 0.63$, $p < 0.001$ and $R^2 = 0.82$, $p < 0.001$, respectively) establishes the importance of considering canopy pigment status (Chl_{Canopy}), as a proxy for canopy photosynthetic potential when modeling carbon assimilation. These results demonstrate that at the start of the growing season, while LAI correlates well with light absorption (fAPAR), the lack of Chl_{Leaf} means that the light is not used for photosynthesis. This will lead to errors in GPP estimates for models that use $FAPAR_{LAI}$, particularly during the early stages of the growing season, when divergence between LAI and Chl_{Leaf} is greatest.

Acknowledgments
The authors gratefully acknowledge the technical field support by Patrick Lee and Paul Bartlett and CFB Borden for hosting the flux site. Funding for the research was provided primarily by Environment Canada. N.F. acknowledges computer resources and research time provided by Northern Michigan University, and H.C. and J.C. thank the National Sciences and Engineering Research Council of Canada for the partial support through a Discovery Grant. In line with the AGU publications data policy, relevant data can be accessed by contacting the corresponding author.

References

Baldocchi, D. (2008), TURNER REVIEW No. 15. "Breathing" of the terrestrial biosphere: Lessons learned from a global network of carbon dioxide flux measurement systems, *Aust. J. Bot.*, *56*, 1–26.

Baldocchi, D., et al. (2001), FLUXNET: A new tool to study the temporal and spatial variability of ecosystem-scale carbon dioxide, water vapor, and energy flux densities, *Bull. Am. Meteorol. Soc.*, *82*, 2415–2434.

Barr, A. G., T. A. Black, E. H. Hogg, N. Kljun, K. Morgenstern, and Z. Nesic (2004), Inter-annual variability in the leaf area index of a boreal aspen-hazelnut forest in relation to net ecosystem production, *Agric. For. Meteorol.*, *126*, 237–255.

Barr, A. G., T. A. Black, E. H. Hogg, T. J. Griffis, K. Morgenstern, N. Kljun, A. Theede, and Z. Nesic (2007), Climatic controls on the carbon and water balances of a boreal aspen forest, 1994–2003, *Global Change Biol.*, *13*, 561–576.

Barr, A. G., et al. (2013), Use of change-point detection for friction-velocity threshold evaluation in eddy-covariance studies, *Agric. For. Meteorol.*, *171*, 31–45.

Buschmann, C. (2007), Variability and application of the chlorophyll fluorescence emission ratio red/far-red of leaves, *Photosynth. Res.*, *92*, 261–271.

Chen, J. M., and J. Cihlar (1995), Plant canopy gap-size analysis theory for improving optical measurements of leaf-area index, *Appl. Opt.*, *34*, 6211–6222.
Chen, J. M., P. S. Plummer, M. Rich, S. T. Gower, and J. M. Norman (1997), Leaf area index measurements, *J. Geophys. Res.*, *102*, 29,429–29,443.
Coops, N. C., T. Hilker, F. G. Hall, C. J. Nichol, and G. G. Drolet (2010), Estimation of light-use efficiency of terrestrial ecosystems from space: A status report, *BioScience*, *60*, 788–797.
Croft, H., J. M. Chen, Y. Zhang, and A. Simic (2013), Modelling leaf chlorophyll content in broadleaf and needle leaf canopies from ground, CASI, Landsat TM 5 and MERIS reflectance data, *Remote Sens. Environ.*, *133*, 128–140.
Croft, H., J. Chen, and T. Noland (2014a), Stand age effects on Boreal forest physiology using a long time-series of satellite data, *For. Ecol. Manage.*, *328*, 202–208.
Croft, H., J. M. Chen, and Y. Zhang (2014b), Temporal disparity in leaf chlorophyll content and leaf area index across a growing season in a temperate deciduous forest, *Int. J. Appl. Earth Obs. Geoinf.*, *33*, 312–320.
Croft, H., J. M. Chen, and Y. Zhang (2014c), The applicability of empirical vegetation indices for determining leaf chlorophyll content over different leaf and canopy structures, *Ecol. Complexity*, *17*, 119–130.
Croft, H., J. Chen, Y. Zhang, A. Simic, T. Noland, N. Nesbitt, and J. Arabian (2015), Evaluating leaf chlorophyll content prediction from multispectral remote sensing data within a physically-based modelling framework, *ISPRS J. Photogramm. Remote Sens.*, *102*, 85–95.
Farquhar, G. D., and T. D. Sharkey (1982), Stomatal conductance and photosynthesis, *Annu. Rev. Plant Physiol.*, *33*, 317–345.
Fensholt, R., I. Sandholt, and M. S. Rasmussen (2004), Evaluation of MODIS LAI, fAPAR and the relation between fAPAR and NDVI in a semi-arid environment using in situ measurements, *Remote Sens. Environ.*, *91*, 490–507.
Froelich, N., H. Croft, J. M. Chen, A. Gonsamo, and R. Staebler (2015), Trends of carbon fluxes and climate over a mixed temperate–boreal transition forest in southern Ontario, Canada, *Agric. For. Meteorol.*, *211–212*, 72–84.
Gitelson, A. A., S. B. Verma, A. Vina, D. C. Rundquist, G. Keydan, B. Leavitt, T. J. Arkebauer, G. G. Burba, and A. E. Suyker (2003), Novel technique for remote estimation of CO_2 flux in maize, *Geophys. Res. Lett.*, *30*, 39–31, doi:10.1029/2002GL016543.
Gitelson, A. A., A. Viña, S. B. Verma, D. C. Rundquist, T. J. Arkebauer, G. Keydan, B. Leavitt, V. Ciganda, G. G. Burba, and A. E. Suyker (2006), Relationship between gross primary production and chlorophyll content in crops: Implications for the synoptic monitoring of vegetation productivity, *J. Geophys. Res.*, *111*, D08S11, doi:10.1029/2005JD006017.
Goldblum, D., and L. S. Rigg (2010), The deciduous forest—Boreal forest ecotone, *Geogr. Compass*, *4*, 701–717.
Gond, V., D. G. G. De Pury, F. Veroustraete, and R. Ceulemans (1999), Seasonal variations in leaf area index, leaf chlorophyll, and water content; Scaling-up to estimate fAPAR and carbon balance in a multilayer, multispecies temperate forest, *Tree Physiol.*, *19*, 673–679.
Gonsamo, A., H. Croft, J. M. Chen, C. Wu, N. Froelich, and R. M. Staebler (2015), Radiation contributed more than temperature to increased decadal autumn and annual carbon uptake of two eastern North America mature forests, *Agric. For. Meteorol.*, *201*, 8–16.
Gower, S. T., C. J. Kucharik, and J. M. Norman (1999), Direct and indirect estimation of leaf area index, (fAPAR), and net primary production of terrestrial ecosystems, *Remote Sens. Environ.*, *70*, 29–51.
Grace, J. (2004), Understanding and managing the global carbon cycle, *J. Ecol.*, *92*, 189–202.
Harris, A., and J. Dash (2010), The potential of the MERIS Terrestrial Chlorophyll Index for carbon flux estimation, *Remote Sens. Environ.*, *114*, 1856–1862.
Hilker, T., N. C. Coops, M. A. Wulder, T. A. Black, and R. D. Guy (2008), The use of remote sensing in light use efficiency based models of gross primary production: A review of current status and future requirements, *Sci. Total Environ.*, *404*, 411–423.
Houborg, R., M. Anderson, and C. Daughtry (2009), Utility of an image-based canopy reflectance modeling tool for remote estimation of LAI and leaf chlorophyll content at the field scale, *Remote Sens. Environ.*, *113*, 259–274.
IPCC (2013), *Climate Change 2013: The Physical Science Basis. Contribution of Working Group I to the Fifth Assessment Report of the Intergovernmental Panel on Climate Change*, edited by T. F. Stock et al., p. 1535, Cambridge Univ. Press, Cambridge, U. K., and New York.
Keenan, T. F., B. Darby, E. Felts, O. Sonnentag, M. Friedl, K. Hufkens, J. O'Keefe, S. Klosterman, J. W. Munger, and M. Toomey (2014), Tracking forest phenology and seasonal physiology using digital repeat photography: A critical assessment, *Ecol. Appl.*, *24*, 1478–1489.
Law, B. E., et al. (2002), Environmental controls over carbon dioxide and water vapor exchange of terrestrial vegetation, *Agric. For. Meteorol.*, *113*, 97–120.
Lee, X. H., J. D. Fuentes, R. M. Staebler, and H. H. Neumann (1999), Long-term observation of the atmospheric exchange of CO_2 with a temperate deciduous forest in southern Ontario, Canada, *J. Geophys. Res.*, *104*(D13), 15975–15984.
Leithead, M., M. Anand, and L. R. Silva (2010), Northward migrating trees establish in treefall gaps at the northern limit of the temperate–boreal ecotone, Ontario, Canada, *Oecologia*, *164*, 1095–1106.
Monteith, J. L. (1972), Solar radiation and productivity in tropical ecosystems, *J. Appl. Ecol.*, *9*, 747–766.
Monteith, J. L. (1977), Climate and the efficiency of crop production in Britain, *Philos. Trans. R. Soc. London, Ser. B*, *281*, 277–294.
Moorthy, I., J. R. Miller, and T. L. Noland (2008), Estimating chlorophyll concentration in conifer needles with hyperspectral data: An assessment at the needle and canopy level, *Remote Sens. Environ.*, *112*, 2824–2838.
Pan, Y., et al. (2011), A large and persistent carbon sink in the world's forests, *Science*, *333*, 988–993.
Peng, Y., A. A. Gitelson, G. Keydan, D. C. Rundquist, and W. Moses (2011), Remote estimation of gross primary production in maize and support for a new paradigm based on total crop chlorophyll content, *Remote Sens. Environ.*, *115*, 978–989.
Peng, Y., A. A. Gitelson, and T. Sakamoto (2013), Remote estimation of gross primary productivity in crops using MODIS 250 m data, *Remote Sens. Environ.*, *128*, 186–196.
Rossini, M., S. Cogliati, M. Meroni, M. Migliavacca, M. Galvagno, L. Busetto, E. Cremonese, T. Julitta, C. Siniscalco, and U. Morra di Cella (2012), Remote sensing-based estimation of gross primary production in a subalpine grassland, *Biogeosciences*, *9*, 2565–2584.
Ruimy, A., B. Saugier, and G. Dedieu (1994), Methodology for the estimation of terrestrial net primary production from remotely sensed data, *J. Geophys. Res.*, *99*, 5263–5283, doi:10.1029/93JD03221.
Ruimy, A., G. Dedieu, and B. Saugier (1996), TURC: A diagnostic model of continental gross primary productivity and net primary productivity, *Global Biogeochem. Cycles*, *10*, 269–285, doi:10.1029/96GB00349.
Running, S. W., R. R. Nemani, F. A. Heinsch, M. Zhao, M. Reeves, and H. Hashimoto (2004), A continuous satellite-derived measure of global terrestrial primary production, *BioScience*, *54*, 547–560.
Staebler, R. M., and D. R. Fitzjarrald (2004), Observing subcanopy CO_2 advection, *Agric. For. Meteorol.*, *122*(3–4), 139–156.
Teklemariam, T., R. M. Staebler, and A. G. Barr (2009), Eight years of carbon dioxide exchange above a mixed forest at Borden, Ontario, *Agric. For. Meteorol.*, *149*(11), 2040–2053.
Webb, E. K., G. I. Pearman, and R. Leuning (1980), Correction of flux measurements for density effects due to heat and water vapour transfer, *Q. J. R. Meteorol. Soc.*, *106*(447), 85–100.
Wellburn, A. R. (1994), The spectral determination of chlorophylls *a* and *b*, as well as total carotenoids, using various solvents with spectrophotometers of different resolution, *J. Plant Physiol.*, *144*, 307–313.

Wu, C., Z. Niu, Q. Tang, and W. Huang (2008), Estimating chlorophyll content from hyperspectral vegetation indices: Modeling and validation, *Agric. For. Meteorol.*, *148*, 1230–1241.

Wu, C., Z. Niu, Q. Tang, W. Huang, B. Rivard, and J. Feng (2009), Remote estimation of gross primary production in wheat using chlorophyll-related vegetation indices, *Agric. For. Meteorol.*, *149*, 1015–1021.

Xiao, X., D. Hollinger, J. Aber, M. Goltz, E. A. Davidson, Q. Zhang, and B. Moore (2004), Satellite-based modeling of gross primary production in an evergreen needleleaf forest, *Remote Sens. Environ.*, *89*, 519–534.

Zha, T. S., et al. (2013), Gross and aboveground net primary production at Canadian forest carbon flux sites, *Agric. For. Meteorol.*, *174*, 54–64.

Zhang, Q., X. Xiao, B. Braswell, E. Linder, F. Baret, and B. Moore Iii (2005), Estimating light absorption by chlorophyll, leaf and canopy in a deciduous broadleaf forest using MODIS data and a radiative transfer model, *Remote Sens. Environ.*, *99*, 357–371.

Zhang, Q., E. M. Middleton, H. A. Margolis, G. G. Drolet, A. A. Barr, and T. A. Black (2009), Can a satellite-derived estimate of the fraction of PAR absorbed by chlorophyll ($fAPAR_{Chl}$) improve predictions of light-use efficiency and ecosystem photosynthesis for a boreal aspen forest?, *Remote Sens. Environ.*, *113*, 880–888.

Zhang, Y., J. M. Chen, and S. C. Thomas (2007), Retrieving seasonal variation in chlorophyll content of overstory and understory sugar maple leaves from leaf-level hyperspectral data, *Can. J. Remote Sens.*, *33*, 406–415.

Zhang, Y., J. M. Chen, J. R. Miller, and T. L. Noland (2008), Leaf chlorophyll content retrieval from airborne hyperspectral remote sensing imagery, *Remote Sens. Environ.*, *112*, 3234–3247.